Rivista Italiana di Paleontologia e Stratigrafia	volume 108	numero 2	tavole 3	pagine 257-273	Luglio 2002

HIGH RESOLUTION CALCAREOUS PLANKTON BIOSTRATIGRAPHY OF THE SERRAVALLIAN SUCCESSION OF THE TREMITI ISLANDS (ADRIATIC SEA, ITALY)

LUCA M. FORESI [1], SERGIO BONOMO [2], ANTONIO CARUSO [2], AGATA DI STEFANO [3], ENRICO DI STEFANO [2], SILVIA M. IACCARINO [4], FABRIZIO LIRER [4], ROBERTO MAZZEI [1], GIANFRANCO SALVATORINI [1] & RODOLFO SPROVIERI [2]

Received July 15, 2001; accepted January 24, 2002

Key words: planktonic foraminifera, calcareous nannofossils, Serravallian, biochronology, Mediterranean.

Riassunto: In questo lavoro vengono presentati i risultati dello studio biostratigrafico ad alta risoluzione dei foraminiferi planctonici e nannofossili calcarei di due sezioni di età Miocene Medio affioranti a S. Nicola, un'isola dell'Arcipelago delle Tremiti (Puglia). I sedimenti studiati fanno parte della Formazione del Cretaccio, un'unità ricca in plancton calcareo che presenta un'evidente ciclicità sedimentaria. Nella successione, infatti, strati di colore biancastro (maggior contenuto in $CaCO_3$) si alternano con altri di colore grigio o rossastro (minor contenuto in $CaCO_3$). Le due sezioni, stratigraficamente sovrapposte, costituiscono una successione di spessore complessivo di 38 m. I campioni sono stati raccolti ad intervalli medi di circa 10-15 cm e per ognuno di essi è stata eseguita l'analisi quantitativa del plancton calcareo rappresentata in curve di frequenza. Le variazioni di abbondanza dei taxa sono state di grande utilità nelle correlazioni e la calibrazione astronomica dei cicli, riconosciuti nelle due sezioni, ha permesso la datazione astrocronologica di tutti i bioeventi in esse contenuti. La successione studiata, di età Serravalliana, abbraccia l'intervallo da 12.60 Ma a 11.12 Ma. Fra gli eventi più significativi si ricordano per i foraminiferi la prima presenza comune (12.34 Ma) e la scomparsa (12.14 Ma) di *Paragloborotalia mayeri*, la scomparsa di *P. partimlabiata* (11.8 Ma), la comparsa dei Neogloboquadrinidi (11.8 Ma), l'ultima presenza comune di *Globigerinoides subquadratus* (11.54 Ma) e la scomparsa di *P. siakensis* (11.21 Ma); per i nannofossili calcarei l'ultima presenza comune di *Calcidiscus premacintyrei* (12.51 Ma), la comparsa (12.57 Ma) e la prima presenza comune (12.34 Ma) di *C. macintyrei*, la prima presenza comune di *Discoaster kugleri* (11.90 Ma), l'ultima presenza comune di *D. kugleri* (11.60 Ma) e l'ultima presenza comune di *Calcidiscus miopelagicus* (11.18 Ma).

Abstract. The planktonic foraminifer and calcareous nannofossil content of two Middle Miocene sections of the Tremiti Islands (Southern Adriatic Sea) have been studied. The two sections are composed of marly limestones rich in calcareous plankton which show cyclic alternations of indurated (higher carbonate content) whitish and less indurated grey or reddish beds. The two sections represent a succession with a total thickness of 38 m. Samples have been collected at a mean spacing of 10-15 cm; qualitative analyses were performed on one sample per meter but quantitative analyses were made for each sample. The abundance fluctuations of several marker species proved to be a very useful tool to correlate the two sections. The astronomical calibration of the sedimentary cycles provided absolute ages for all the recognised calcareous plankton bioevents.

Introduction

More than ten years ago, some of the writers studied the Neogene sediments of the Tremiti Islands. Up to now some results have been published by Bossio et al. (1992), Foresi et al. (1998) and Iaccarino et al. (2001) and a detailed paper focused on the taxonomy and stratigraphical distribution of calcareous plankton has been recently submitted (Foresi et al. in press). During the fieldwork of the last decade the rhythmic alternation of whitish, grey or rarely reddish beds has been observed, but its meaning was not investigated.

During the last decade cyclostratigraphy and astrochronological calibration became new methodological approaches for the construction of high resolution timescales. In fact, the astronomical timescale (ATS) for the Plio-Pleistocene (Hilgen 1991 a, b) has been incorporated in the geological timescale (Berggren et al. 1995). More recently further progress has been made in extending this timescale to the Late Miocene Epoch (Hilgen et al. 1995, 2000; Shackleton & Crowhurst 1997).

In the light of these new findings, the lithological cyclicity of the Miocene succession outcropping in the Tremiti Islands has been studied. The astronomical tuning of the lithological record has been performed by Lirer et al. (2002), thus providing astronomical ages for calcareous plankton bioevents. This paper presents the high resolution calcareous plankton biostratigraphy of

[1] Dipartimento di Scienze della Terra, Università di Siena, Via Laterina 8, 53100 Siena, Italy. foresi@unisi.it
[2] Dipartimento di Geologia e Geodesia, Università di Palermo, Corso Tukory 131, 90134 Palermo, Italy
[3] Dipartimento di Scienze Geologiche - Università di Catania, Corso Italia 55, 95129 Catania, Italy
[4] Dipartimento di Scienze della Terra, Università di Parma, Parco Area delle Scienze 157/A, 43100 Parma, Italy

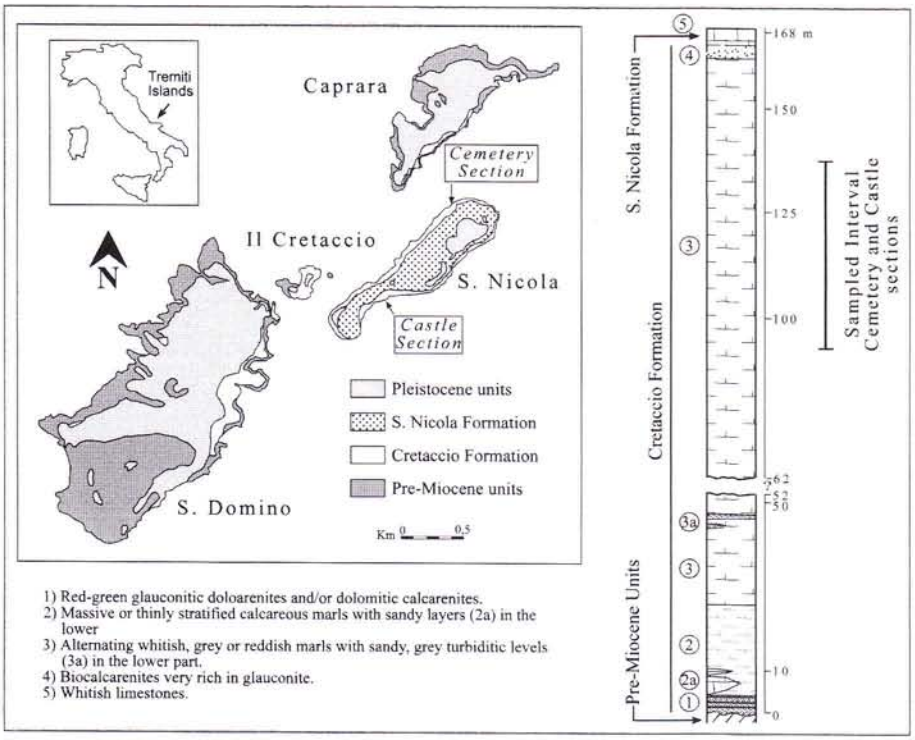

Fig. 1 - Location map with major geological units and formations of the Tremiti Islands and synthetic lithostratigraphic log of the Miocene succession.

the S. Nicola composite section which ecompasses the choronological interval between 12.60 Ma and 11.12 Ma.

Geological setting

The Tremiti archipelago (Fig. 1) is made up of the three islands S. Domino, S. Nicola and Caprara and the two islets (Pianosa and Il Cretaccio). It is located about 20 km off the north coast of Gargano (Apulia), at the northern margin of the Apulian platform and belongs to the Adriatic domain (Gambini & Tozzi 1996).

The geology of the Tremiti Islands has been documented by Tellini (1890), Bassani (1907), Squinabol (1908), Checchia Rispoli (1926, 1928), Baldacci (1953), Pasa (1953), Selli (1971), and more recently by Pampaloni (1988) and Cotecchia et al. (1996). The stratigraphy of the islands was established by Selli (1971) who distinguished 3 pre-Neogene formations outcropping mainly in S. Domino and Caprara and 2 marine Neogene formations:

Fig. 2 - Sampling trajectories of the Cemetery Section, S. Nicola Island.

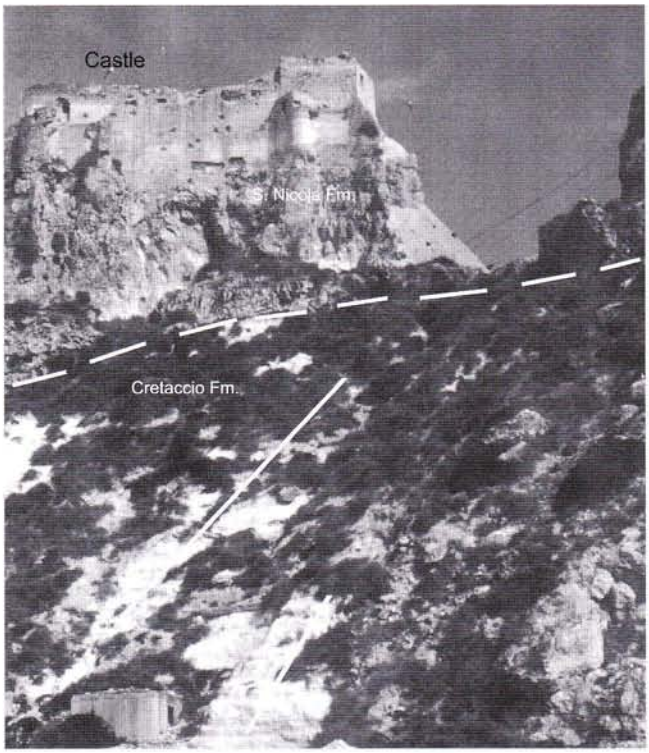

Fig. 3 - Sampling trajectories of the Castle Section, S. Nicola Island.

- the Cretaccio Formation (Fm), lying with angular unconformity on the pre-Miocene units and mainly composed of yellowish marls and calcareous marls;

- the S. Nicola Fm, lying on the Cretaccio Formation, consisting of dolomitic limestones and biocalcarenites.

The marine formations are capped by continental conglomerates, strips of loess and calcareous crust (caliche) of middle to late Pleistocene age (Selli 1971; Cotecchia et al. 1996).

The Miocene succession shows a general SE dipping and an intense faulting and fracturation due to prevailing extensional tectonics. The major faults are post-Miocene in age and have NW- SE and E-W trends.

A synthetic stratigraphic log of the Cretaccio Fm, which is described in Iaccarino et al. (2001), is shown in Fig. 1. Iaccarino et al. (2001) and Foresi et al. (in press) assigned the Cretaccio Fm to the *Praeorbulina glomerosa* s.l. Zone - *Globorotalia conomiozea* Zone interval of the Iaccarino & Salvatorini (1982) and Iaccarino (1985) planktonic foraminiferal zonal schemes and to the *Discoaster exilis-Sphenolithus heteromorphus* Zone - *Amaurolithus delicatus-A. amplificus* Zone interval of the nannofossil zonation of Mazzei (in Iaccarino et al. 2001) and the lower part of the S. Nicola Fm to the foraminiferal "Non distinctive" Zone and to the nannofossil *A. delicatus-A. amplificus* Zone. The geochronological assignment of the Cretaccio Fm is Langhian to Messinian in age and the lower part of S. Nicola Fm is Messinian in age.

The studied section

The investigated S. Nicola composite section is entirely comprised in the Cretaccio Fm cropping out on S. Nicola Island. It consists of the Cemetery and the Castle sections (Fig. 1). These two sections have been selected on the basis of the lithological and biostratigraphic data described by Iaccarino et al. (2001). In fact, the Cemetery and Castle sections are very close to the Section 9 and 10 of the mentioned work. The Cemetery section (Fig. 2), 19 m-thick, is located on the NW coast of the island, below the cemetery and the sample trajectory lies on the right side of a clearly visible normal fault with apenninic trend. The Castle section (Fig. 3), 26 m-thick, is located on the SE coast, below the castle and consists of two segments of 7.61 and 18.42 m, separated by a shear plane (Fig. 4). The composite section has a total thickness of 38 m.

The sedimentary record of S. Nicola composite section consists of a quasi-regular alternation of indurated, whitish coloured, $CaCO_3$-rich marly beds and greycoloured less indurated, $CaCO_3$-poor marly beds. Red coloured, $CaCO_3$-poor marls at times replace the grey marls. The marly limestones are 0.25-1 meter thick, while the red and grey marls range from a few centimetres up to 80 cm. Bioturbation is present throughout the section and, locally, fossil remains like *Flabellipecten* and *Neopycnodonte* are very abundant.

The cyclostratigraphic study carried out on the S. Nicola composite section has been performed by Lirer et al. (2002). The lithologic cycles are not evenly distributed throughout the section but reveal a distinct pattern and frequency. In particular, in the Castle section the lithologic cyclicity is not visible from 9 m to 15.30 m because of poor exposure of the outcrop, while it is again recognisable in the uppermost 4 m of the section. In the Cemetery section the cyclicity is clearly evident throughout the whole section and the thickness of the sedimentary cycles is more regular than in the Castle section. Lirer et al. (2002) recorded 52 cycles spanning 1.5 My, from 12.60 Ma to 11.12 Ma.

Paleomagnetic and stable isotope analyses carried out on some samples revealed that the magnetisation of the sediments and the overgrowth of the foraminiferal tests respectively prevented to obtain reliable results.

Biostratigraphy and biochronology

Planktonic foraminifera. The foraminiferal analysis was carried out on 182 and 251 samples from the Cemetery (Tab. 1) and Castle (Tab. 2) sections respectively, at a mean spacing of about 10-15 cm. Preservation is generally good and on average is better in the grey/red layers than in the whitish indurated layers where sometimes the foraminiferal tests show overgrowth. Samples

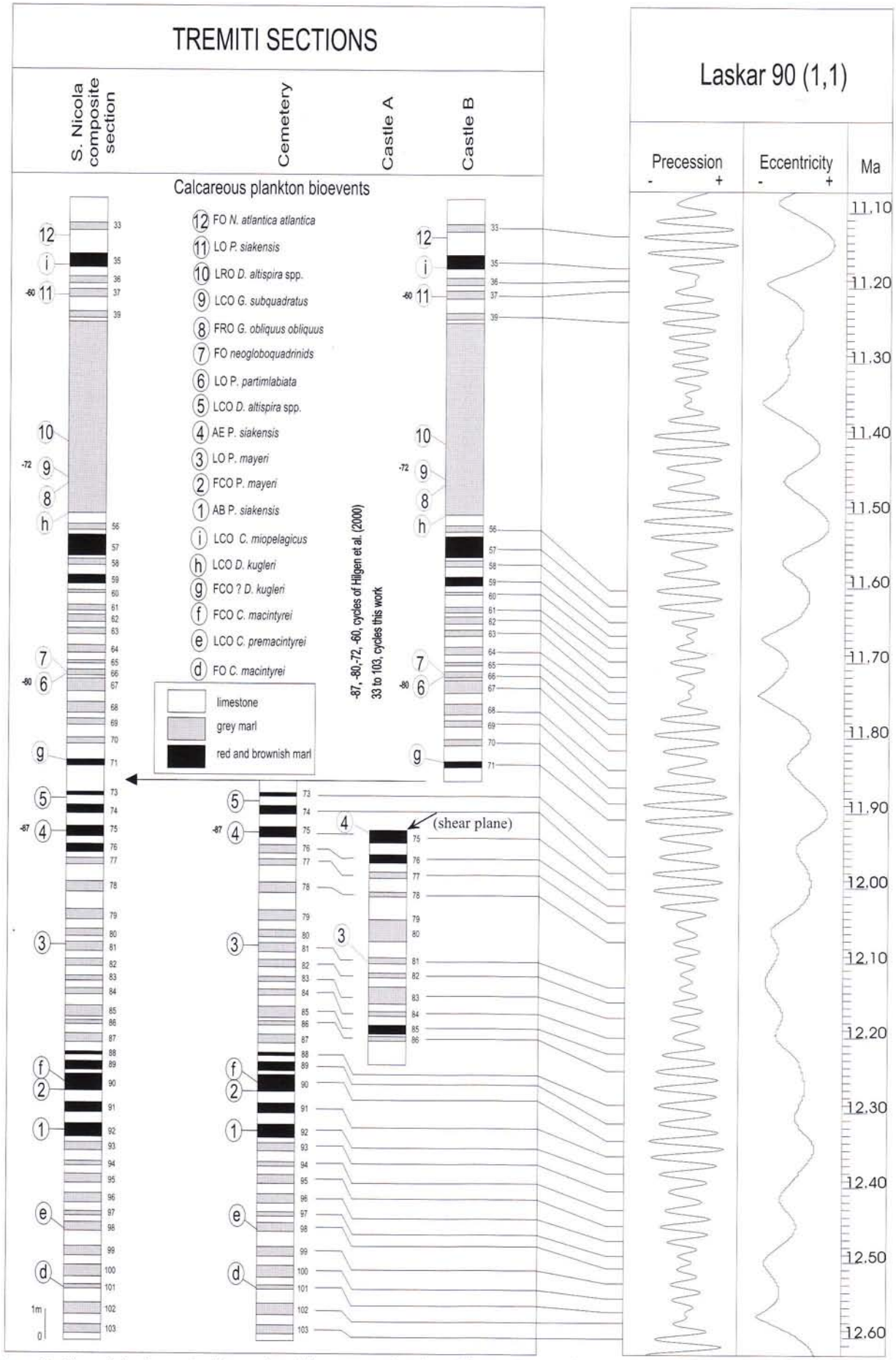

Fig. 4 - Position of the first order biostratigraphic events and tuning of the sections to the astronomic solution of Laskar et al. (1993).

Sample number	depth (m)	Sample number	depth (m)	Sample number	depth (m)	Sample number	depth (m)
TTA - 0	0,00	TTA - 46	4,60	TTA - 92	9,40	TTA - 193	13,90
TTA - 1	0,10	TTA - 47	4,70	TTA - 93	9,50	TTA - 195	14,00
TTA - 2	0,20	TTA - 48	4,80	TTA - 94	9,60	TTA - 197	14,10
TTA - 3	0,30	TTA - 49	4,90	TTA - 95	9,70	TTA - 199	14,20
TTA - 4	0,40	TTA - 50	5,00	TTA - 96	9,80	TTA - 200	14,35
TTA - 5	0,50	TTA - 51	5,10	TTA - 97	9,90	TTA - 202	14,55
TTA - 6	0,60	TTA - 52	5,20	TTA - 98	10,00	TTA - 203	14,65
TTA - 7	0,70	TTA - 53	5,30	TTA - 99	10,10	TTA - 204	14,75
TTA - 8	0,80	TTA - 54	5,40	TTA - 100	10,20	TTA - 206	14,85
TTA - 9	0,90	TTA - 55	5,70	TTA - 101	10,30	TTA - 207	14,95
TTA - 10	1,00	TTA - 56	5,80	TTA - 102	10,40	TTA - 208	15,05
TTA - 9	1,10	TTA - 57	5,90	TTA - 103	10,50	TTA - 209	15,15
TTA - 8	1,20	TTA - 58	6,00	TTA - 104	10,60	TTA - 210	15,25
TTA - 7	1,30	TTA - 59	6,10	TTA - 105	10,70	TTA - 211	15,35
TTA - 6	1,40	TTA - 60	6,20	TTA - 106	10,80	TTA - 212	15,45
TTA - 15	1,50	TTA - 61	6,30	TTA - 107	10,90	TTA - 213	15,55
TTA - 14	1,60	TTA - 62	6,40	TTA - 108	11,00	TTA - 214	15,65
TTA - 13	1,70	TTA - 63	6,50	TTA - 109	11,10	TTA - 215	15,75
TTA - 12	1,80	TTA - 64	6,60	TTA - 110	11,20	TTA - 216	15,85
TTA - 19	1,90	TTA - 65	6,70	TTA - 111	11,30	TTA - 218	15,95
TTA - 20	2,00	TTA - 66	6,80	TTA - 112	11,40	TTA - 219	16,05
TTA - 19	2,10	TTA - 67	6,90	TTA - 113	11,50	TTA - 220	16,15
TTA - 22	2,20	TTA - 68	7,00	TTA - 114	11,60	TTA - 221	16,25
TTA - 23	2,30	TTA - 69	7,10	TTA - 115	11,70	TTA - 222	16,35
TTA - 24	2,40	TTA - 70	7,20	TTA - 116	11,80	TTA - 223	16,45
TTA - 25	2,50	TTA - 71	7,30	TTA - 117	11,90	TTA - 224	16,55
TTA - 26	2,60	TTA - 72	7,40	TTA - 118	12,00	TTA - 225	16,65
TTA - 25	2,70	TTA - 73	7,50	TTA - 119	12,10	TTA - 226	16,75
TTA - 24	2,80	TTA - 74	7,60	TTA - 120	12,20	TTA - 227	16,85
TTA - 29	2,90	TTA - 75	7,70	TTA - 121	12,30	TTA - 228	16,95
TTA - 30	3,00	TTA - 76	7,80	TTA - 122	12,40	TTA - 229	17,05
TTA - 29	3,10	TTA - 77	7,90	TTA - 123	12,50	TTA - 230	17,15
TTA - 28	3,20	TTA - 78	8,00	TTA - 124	12,60	TTA - 231	17,25
TTA - 27	3,30	TTA - 79	8,10	TTA - 125	12,70	TTA - 232	17,35
TTA - 26	3,40	TTA - 80	8,20	TTA - 126	12,80	TTA - 233	17,45
TTA - 25	3,50	TTA - 81	8,30	TTA - 127	12,90	TTA - 234	17,55
TTA - 24	3,60	TTA - 82	8,40	TTA - 128	13,00	TTA - 235	17,65
TTA - 23	3,70	TTA - 83	8,50	TTA - 129	13,10	TTA - 236	17,75
TTA - 38	3,80	TTA - 84	8,60	TTA - 130	13,20	TTA - 237	17,85
TTA - 39	3,90	TTA - 85	8,70	TTA - 184	13,30	TTA - 238	17,95
TTA - 40	4,00	TTA - 86	8,80	TTA - 185	13,40	TTA - 239	18,05
TTA - 41	4,10	TTA - 87	8,90	TTA - 186	13,50	TTA - 240	18,15
TTA - 42	4,20	TTA - 88	9,00	TTA - 187	13,60	TTA - 241	18,25
TTA - 43	4,30	TTA - 89	9,10	TTA - 189	13,70	TTA - 242	18,35
TTA - 44	4,40	TTA - 90	9,20	TTA - 191	13,80	TTA - 243	18,45
TTA - 45	4,50	TTA - 91	9,30				

Tab. 1 - List and depth of the investigated samples of the Cemetery section. Sample depth of Cemetery section is the same as in the composite section.

Sample number	depth (m) composite section	depth (m) Castle	Sample number	depth (m) composite section	depth (m) Castle	Sample number	depth (m) composite section	depth (m) Castle
TTAA - 112	18,60	12,50	TTAA - 174	25,09	18,83	TTAA - 236	31,29	25,03
TTAA - 113	18,70	12,60	TTAA - 175	25,19	18,93	TTAA - 237	31,39	25,13
TTAA - 114	18,80	12,70	TTAA - 176	25,29	19,03	TTAA - 238	31,49	25,23
TTAA - 115	18,90	12,80	TTAA - 177	25,39	19,13	TTAA - 239	31,59	25,33
TTAA - 116	19,00	12,90	TTAA - 178	25,49	19,23	TTAA - 240	31,69	25,43
TTAA - 117	19,10	13,00	TTAA - 179	25,59	19,33	TTAA - 241	31,79	25,53
TTAA - 118	19,20	13,10	TTAA - 180	25,69	19,43	TTAA - 242	31,89	25,63
TTAA - 119	19,32	13,22	TTAA - 181	25,79	19,53	TTAA - 243	31,99	25,73
TTAA - 120	19,44	13,32	TTAA - 182	25,89	19,63	TTAA - 244	32,09	25,83
TTAA - 121	19,56	13,42	TTAA - 183	25,99	19,73	TTAA - 245	32,19	25,93
TTAA - 122	19,68	13,52	TTAA - 184	26,09	19,83	TTAA - 246	32,29	26,03
TTAA - 123	19,80	13,62	TTAA - 185	26,19	19,93	TTAA - 247	32,39	26,13
TTAA - 124	19,94	13,76	TTAA - 186	26,29	20,03	TTAA - 248	32,49	26,23
TTAA - 125	20,08	13,86	TTAA - 187	26,39	20,13	TTAA - 249	32,59	26,33
TTAA - 126	20,22	13,96	TTAA - 188	26,49	20,23	TTAA - 250	32,69	26,43
TTAA - 127	20,37	14,11	TTAA - 189	26,59	20,33	TTAA - 251	32,79	26,53
TTAA - 128	20,47	14,21	TTAA - 190	26,69	20,43	TTAA - 252	32,89	26,63
TTAA - 129	20,57	14,31	TTAA - 191	26,79	20,53	TTAA - 253	32,99	26,73
TTAA - 130	20,67	14,41	TTAA - 192	26,89	20,63	TTAA - 254	33,09	26,83
TTAA - 131	20,77	14,51	TTAA - 193	26,99	20,73	TTAA - 255	33,19	26,93
TTAA - 132	20,87	14,61	TTAA - 194	27,09	20,83	TTAA - 256	33,29	27,03
TTAA - 133	20,97	14,71	TTAA - 195	27,19	20,93	TTAA - 257	33,39	27,13
TTAA - 134	21,07	14,81	TTAA - 196	27,29	21,03	TTAA - 258	33,49	27,23
TTAA - 135	21,17	14,91	TTAA - 197	27,39	21,13	TTAA - 259	33,59	27,33
TTAA - 136	21,27	15,01	TTAA - 198	27,49	21,23	TTAA - 260	33,69	27,43
TTAA - 137	21,37	15,11	TTAA - 199	27,59	21,33	TTAA - 261	33,79	27,53
TTAA - 138	21,47	15,21	TTAA - 200	27,69	21,43	TTAA - 262	33,89	27,63
TTAA - 139	21,57	15,31	TTAA - 201	27,79	21,53	TTAA - 277	33,99	27,73
TTAA - 140	21,67	15,41	TTAA - 202	27,89	21,63	TTAA - 278	34,09	27,83
TTAA - 141	21,77	15,51	TTAA - 203	27,99	21,73	TTAA - 279	34,19	27,93
TTAA - 142	21,87	15,61	TTAA - 204	28,09	21,83	TTAA - 280	34,29	28,03
TTAA - 143	21,97	15,71	TTAA - 205	28,19	21,93	TTAA - 281	34,39	28,13
TTAA - 144	22,07	15,81	TTAA - 206	28,29	22,03	TTAA - 282	34,49	28,23
TTAA - 145	22,17	15,91	TTAA - 207	28,39	22,13	TTAA - 283	34,59	28,33
TTAA - 146	22,27	16,01	TTAA - 208	28,49	22,23	TTAA - 284	34,69	28,43
TTAA - 147	22,37	16,11	TTAA - 209	28,59	22,33	TTAA - 285	34,79	28,53
TTAA - 148	22,47	16,21	TTAA - 210	28,69	22,43	TTAA - 286	34,89	28,63
TTAA - 149	22,57	16,31	TTAA - 211	28,79	22,53	TTAA - 287	34,99	28,73
TTAA - 150	22,67	16,41	TTAA - 212	28,89	22,63	TTAA - 288	35,09	28,83
TTAA - 151	22,77	16,51	TTAA - 213	28,99	22,73	TTAA - 289	35,19	28,93
TTAA - 152	22,89	16,63	TTAA - 214	29,09	22,83	TTAA - 290	35,29	29,03
TTAA - 153	22,99	16,73	TTAA - 215	29,19	22,93	TTAA - 291	35,39	29,13
TTAA - 154	23,09	16,83	TTAA - 216	29,29	23,03	TTAA - 292	35,49	29,23
TTAA - 155	23,19	16,93	TTAA - 217	29,39	23,13	TTAA - 293	35,59	29,33
TTAA - 156	23,29	17,03	TTAA - 218	29,49	23,23	TTAA - 294	35,69	29,43
TTAA - 157	23,39	17,13	TTAA - 219	29,59	23,33	TTAA - 295	35,79	29,53
TTAA - 158	23,49	17,23	TTAA - 220	29,69	23,43	TTAA - 296	35,89	29,63
TTAA - 159	23,59	17,33	TTAA - 221	29,79	23,53	TTAA - 297	35,99	29,73
TTAA - 160	23,69	17,43	TTAA - 222	29,89	23,63	TTAA - 298	36,09	29,83
TTAA - 161	23,79	17,53	TTAA - 223	29,99	23,73	TTAA - 299	36,19	29,93
TTAA - 162	23,89	17,63	TTAA - 224	30,09	23,83	TTAA - 300	36,29	30,03
TTAA - 163	23,99	17,73	TTAA - 225	30,19	23,93	TTAA - 301	36,39	30,13
TTAA - 164	24,09	17,83	TTAA - 226	30,29	24,03	TTAA - 302	36,49	30,23
TTAA - 165	24,19	17,93	TTAA - 227	30,39	24,13	TTAA - 303	36,59	30,33
TTAA - 166	24,29	18,03	TTAA - 228	30,49	24,23	TTAA - 304	36,69	30,43
TTAA - 167	24,39	18,13	TTAA - 229	30,59	24,33	TTAA - 305	36,79	30,53
TTAA - 168	24,49	18,23	TTAA - 230	30,69	24,43	TTAA - 306	36,89	30,63
TTAA - 169	24,59	18,33	TTAA - 231	30,79	24,53	TTAA - 307	36,99	30,73
TTAA - 170	24,69	18,43	TTAA - 232	30,89	24,63	TTAA - 308	37,09	30,83
TTAA - 171	24,79	18,53	TTAA - 233	30,99	24,73	TTAA - 309	37,19	30,93
TTAA - 172	24,89	18,63	TTAA - 234	31,09	24,83	TTAA - 310	37,29	31,03
TTAA - 173	24,99	18,73	TTAA - 235	31,19	24,93	TTAA - 311	37,39	31,13

Tab. 2 - List of the investigated samples of the Castle section.

were first dehydrated in oven at 40 degrees, subsequently disaggregated in distilled water and washed with a 63 μm sieve. Fig. 5 shows the quantitative distribution pattern of 14 planktonic foraminiferal categories having biostratigraphic significance. The patterns are based on counting of about 300 specimens of all planktonic species from splits of the >125 μm fraction. A qualitative analysis based on more detailed surveying of the >63 μm fraction, has been performed every meter. Taxon abundance is expressed as percentage of the total assemblage. Fluctuations and distributions of the selected planktonic foraminifera are described and related to the astronomical tuning.

Globigerinoides obliquus obliquus Bolli (Pl. 1, figs. 1-3)

The distribution pattern of this taxon is very discontinuous. The curve (Fig. 5) shows two major influxes characterised by high percentages values (5-10%). The first one between 13 m and 15 m and the second one, from 28.69 m up to the top of the section. At the base of the second interval the First Regular Occurrence (FRO) of this species occurs which shows a progressive increase in abundance.

Globigerinoides subquadratus Brönnimann (Pl. 1, figs. 4-6)

This taxon shows a discontinuous distribution through rhythmic abundance peaks (>40%). In the upper part of the range *G. subquadratus* shows a more continuous presence, with percentages lower than previous ones. The Last Common Occurrence (LCO) of the species, which is a first order biostratigraphic event, occurs at 28.89 m (at 11.54 Ma). This event slightly postdates the FRO of *G. obliquus obliquus* and coincides with the end of the first influx of neogloboquadrinids as in M. Gibliscemi section (Hilgen et al. 2000).

Neogloboquadrinids (Pl. 1, figs. 7-16)

In our succession we distinguished *Neogloboquadrina acostaensis* (Blow) (Pl. 1, figs. 7-8), *N. atlantica praeatlantica* Foresi, Iaccarino & Salvatorini (Foresi et al.

2002b) (Pl. 1, figs. 9-16) and *N. atlantica atlantica* (Berggren). The first representative is *N. atlantica praeatlantica* which includes the forms previously reported as *N. continuosa* (Foresi et al. 1998) and *N. atlantica* (small sized) (Hilgen et al., 2000). A complete description and revision of the taxonomy of this new subspecies is given by Foresi et al. (2002b). *N. acostaensis* is the second representative; in our concept this taxon comprises forms with 4 - 5 chambers in the last whorl. The 4-chambered morphotypes occur within the neogloboquadrinid population in the lower part of its range. The 4-chambered type of Hilgen et al. (2000) is included in *N. acostaensis*. *N. atlantica atlantica* is the third representative of this group. Our specimens well correspond to the diagnostic features of the holotype, particularly in terms of shape and texture of the test.

The First Occurrence (FO) of the neogloboquadrinids is recorded at 22.17 m, in cycle 66 (dated at 11.8 Ma). In the same cycle have been recorded both *N. atlantica praeatlantica* and *N. acostaensis* s.s. FOs.

The synchroneity of these events have been already documented by Hilgen et al. (2000). The origin of the neogloboquadrinids group is still an unsolved question. The earliest neogloboquadrinids are recorded from the late Middle Miocene in the north Atlantic region (Hilgen et al. 2000 and reference therein). These earliest specimens migrated into the Mediterranean from regions north of Iceland. In fact, the earliest spreading of this group in the tropical region occurs in the early-Late Miocene at 9.89 Ma (Turco et al. in press) or at 9.82 Ma (Chaisson & Pearson 1997)

Recently, in Leg 162-Site 982B (north Atlantic, Rockall Plateau), the FO of *N. atlantica praeatlantica* (unpublished data) has been recorded in the *Bolboforma badenensis* Zone between 11.9 and 12.6 Ma (Spiegler 1999). This datum supports that the appearance of *N. atlantica praeatlantica* in the north Atlantic regions is older than in the Mediterranean.

A paracme interval in the distribution range of neogloboquadrinids has been observed from about 28.89 m (11.54 Ma) to about 34.5 m (11.21 Ma). The base of this paracme interval almost coincides with the LCO of *G. subquadratus* and with the FRO of *G. obliquus obliquus*. A second influx of neogloboquadrinids, correlatable to that recorded by Hilgen et al. (2000), is very close to the *N. atlantica atlantica* FO which occurs at 36.39 m (at 11.16 Ma). The arrival of the second influx of neogloboquadrinids closely postdates the Last Occurrence (LO) of *Paragloborotalia siakensis* and the beginning of the saw teeth distribution of *G. obliquus obliquus*.

From the base of their distribution up to the base of the paracme interval the neogloboquadrinids are randomly coiled. Within the paracme, the specimens are very rare but right coiling seems to prevail. The right coiling starts to dominate above the paracme interval at 11.25 Ma at the same age than that reported in Hilgen et al. (2000) (Fig. 5).

Catapsydrax parvulus Bolli, Loeblich & Tappan (Pl. 1, figs. 17-18)

During the study of the Miocene succession of the Tremiti Islands, Foresi et al. (in press) highlighted that there are no differences between *Globorotaloides falconarae* Giannelli & Salvatorini and *C. parvulus*. *Consequently*, the opinion of Zachariasse (1992) and Krijgsman et al. (1995, 1999) that *G. falconarae* is a junior synonym of *C. parvulus* is followed here.

In our succession the first rare specimens of *C. parvulus* are recorded at 21.77 m (dated at 11.83 Ma) (Fig. 5). This level slightly predates the FCO of the taxon that almost coincides with the neogloboquadrinids FO. The size of the taxon is variable, ranging from small (about 130 μm, like the typical *C. parvulus*) to large specimens (about 250 μm). The large specimens closely resemble *Globoquadrina* sp. 1 of Hilgen et al. (2000).

Paragloborotalia partimlabiata (Ruggieri & Sprovieri) (Pl. 2, figs. 1-7)

This taxon is present from the base of the section with high percentages (30-50%) and its FO has been recorded in the Ras il-Pellegrin section (Malta) at 12.62 Ma (Foresi et al. 2002a) one cycle below the base of the S. Nicola section. The LO of the species occurs at 22.17 m (at 11.8 Ma) and is synchronous with the FO of the neogloboquadrinids. According to Hilgen et al. (2000) *P. partimlabiata* occurs up to 9.91 Ma. In our opinion they do not correspond to the typical forms because they are smaller, with less inflated chambers and more radial sutures than typical *P. partimlabiata* (see also Foresi et al. in press) and we labelled them *P.* cf. *partimlabiata* (Fig. 5, Pl. 2, figs. 8-11). However, our LO of *P. partimlabiata* is well recognisable in the distribution pattern of Hilgen et al. (2000) because it coincides with the sharp drop in abundance of the taxon which realises very close to the neogloboquadrinids FO.

Paragloborotalia mayeri (Cushman & Ellisor) (Pl. 2, figs. 12-16)

Following the concept of Blow (1969) we distinguished *P. mayeri* from *P. siakensis* as Cita et al. (1978), Salvatorini & Cita (1979), Iaccarino (1985), Foresi et al. (1998, 2002a). According to Bolli & Saunders (1982, 1985) and Hilgen et al. (2000) the two taxa are co-specific. The first specimens of this taxon show some features (like the shape of the test and the aperture) similar to *P. partimlabiata*. Therefore, Foresi et al. (in press) inferred that *P. mayeri* could be evolved from *P. partimlabiata*. *P. mayeri* shows a very short distribution pattern, with a mean percentage lower than 15%. The FO of this taxon is a event difficult to be detected. It has been recorded only through the qualitative analysis in Malta at 12.39 Ma (Foresi et al. 2002a). On the contrary,

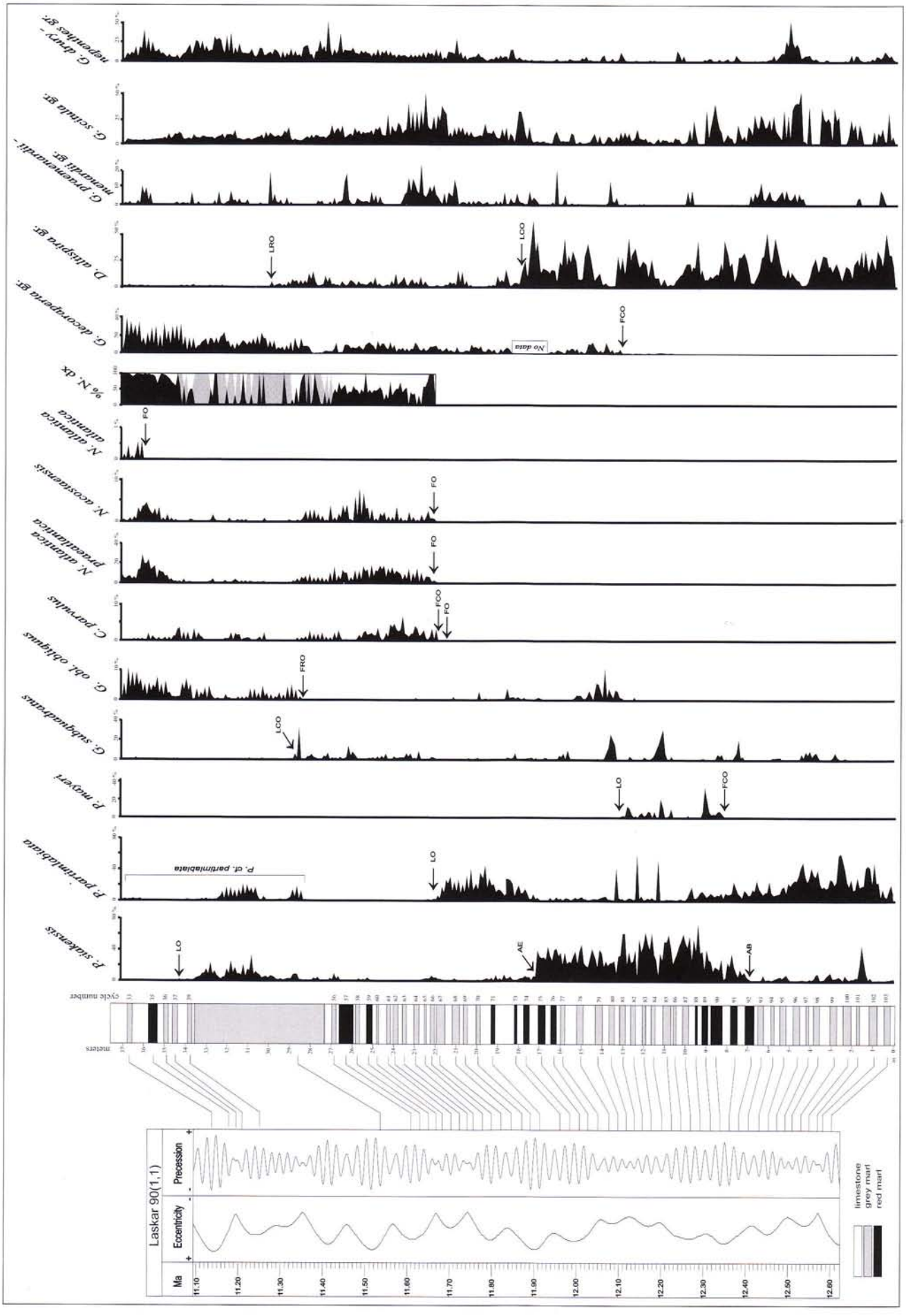

Fig. 5 - Quantitative distribution of selected planktonic foraminifera. FO: First Occurrence; LO: Last Occurrence; FCO: First Common Occurrence; LCO: Last Common Occurrence; LRO: First Regular Occurrence; LRO: Last Regular Occurrence; AB: Acme Base; AE: Acme End. Grey colour in the coiling trend of the neogloboquadrinids represents the intervals without neogloboquadrinids.

the FCO of the taxon is an easily recognisable event and it has been recorded in the S. Nicola section at 8.10 m in cycle 90 (12.34 Ma). The LO of the taxon in cycle 81 (12.14 Ma) practically coincides with the first influx of *Globigerinoides obliquus obliquus* and with the FCO of *Globoturborotalia decoraperta* gr. (Fig. 5).

Paragloborotalia siakensis (LeRoy) (Pl. 3, figs. 2-16)

In the counting of *P. siakensis* we included typical forms of *P. siakensis* and 4-chambered small-sized specimens (see Bolli & Saunders 1982). Both forms are always present in the section up to the LO of the species recorded in cycle 37 (at 12.21 Ma). The distribution pattern shows an acme interval between 6.9 m (dated at 12.38 Ma) and 17.2 m (dated at 12.00 Ma). Below and above this interval *P. siakensis* is rare. Fig. 5 shows that *P. siakensis* and *P. partimlabiata* are two vicariant species both in long and short distribution: the acme of *P. siakensis* between cycle 92 and 75 and three peaks between cycles 80-85 coincide with the low frequency of *P. partimlabiata*.

Globorotalia praemenardii-menardii group (Pl. 1, figs.19-20; Pl. 3, fig.1)

Globorotalia praemenardii praemenardii Cushman & Stainfort (Pl. 1, figs.19-20), *Globorotalia* aff. *menardii* (Parker, Jones & Brady) (Pl. 3, fig.1) and *Globorotalia menardii* s.l. are included in this taxonomic unit. These taxa have been distinguished only through qualitative analysis.

All taxa have a low trochospiral test with a peripheral keel; 5-6 chambers in the last whorl, a low arched slit-like aperture at the base of the last chamber, and on the spiral side the sutures are strongly curved. The three taxa differ from each other in the development of the peripheral keel, the shape of the chambers in spiral view, and finally in the development of limbate spiral and intercameral sutures. *G. praemenardii praemenardii* shows a narrow keel, a slow increase in chamber size and a not limbate spiral suture; *G.* aff. *menardii* has a more prominent keel, a slow increase in chamber size and a slight limbate spiral suture; *G. menardii* s.l. shows semicircular outline of the chambers, a prominent keel and a limbate spiral suture. *G.* aff. *menardii* corresponds to *G.* ex gr. *cultrata* of Giannelli & Salvatorini (1975) and Cita et al. (1978) and probably to *G. menardii* form 2 and 3 of Tjalsma (1971) and Zachariasse (1975).

The abundance pattern of these globorotalias is not continuous, the mean percentages are lower than 5-6%. Higher percentage (10-15%) were observed between 6.9 and 17.2 meters below and above the acme of *P. siakensis*.

Globoturborotalia decoraperta group

This taxonomic unit including *Globoturborotalia decoraperta* (Takayanagi & Saito), *G. apertura* and *G. woodi* (Jenkins) is rare in the lower part of the section, becomes common from cycle 90 where the FCO of *G. decoraperta* gr. has been recognised. This event occurs in the same cycle as the *P. mayeri* LO. The FCO of *G. decoraperta* gr. is followed by a further increase in abundance just below the LCO of *G. subquadratus* and FRO of *G. obliquus obliquus*. The second increase of *G. decoraperta* gr. associated with the FRO of *G. obliquus obliquus* is well correlatable to the increase of *G. obliquus obliquus-G. apertura* gr. recorded in M. Gibliscemi section (Sicily) by Hilgen et al. (2000).

Dentoglobigerina altispira group

Dentoglobigerina altispira gr., which includes mainly *D. altispira altispira* and *D. altispira globosa*, is very abundant (with percentage > 50%) from the base of the section up to 17.75 m (cycle 74) where its LCO is well detectable. Upwards, *D. altispira* gr. is present with lower percentages (< 20%) and at 30.01 m (dated at 11.47 Ma) its Last Regular Occurrence (LRO) is recorded. Only rare specimens are detectable in the upper part of the succession.

Calcareous nannofossils. The calcareous nannofossil study is based on quantitative analysis of 182 samples from the Cemetery section and 125 samples from the Castle section where particular emphasis has given to the crucial intervals. Qualitative analysis has also been performed on one sample per meter. Smear slides were prepared from unprocessed sediments following standard techniques. To obtain the distribution patterns of selected calcareous nannofossil taxa, light microscope analyses were performed (transmitted light and crossed nicols) at about 1000X magnification. Abundance data were collected using methodology described by Backman & Shackleton (1983), Rio et al. (1990) and extensively used in Mediterranean and extra-Mediterranean quantitative biostratigraphic studies of Neogene marine records; ODP sequences and land sections; (Raffi & Flores 1995; Raffi et al. 1995; Fornaciari et al. 1996; Backman & Raffi 1997; Di Stefano 1998; Hilgen et al. 2000).

The following counting methods were used:

1) Index species versus a prefixed number of taxonomically related forms;

2) Number of specimens of an index species or genus in a prefixed area of the slide (4.52 mm^2).

Method 1 was adopted to detect abundance patterns of *Calcidiscus premacintyrei* and *C. macintyrei* (within 30 to 50 *Calcidiscus*), *Coccolithus miopelagicus* (within 100 *Coccolithus*), *Helicosphaera walbersdorfensis* and *H. stalis* (within 100 helicoliths).

Method 2 was adopted to detect the abundance patterns of total *Discoaster* and *D. kugleri*.

Calcareous nannofossils are generally abundant to common throughout both sections. Large to medium

size placoliths of the genera *Calcidiscus, Coccolithus, Dictyococcites* and *Reticulofenestra* are the most common components of the nannofossil assemblages in both sections. Reworked taxa occur throughout the sections in low frequency.

Preservation is moderate to good in the Castle section, but it is poor to very poor in the Cemetery section, with partially dissolved and/or overgrown assemblages. Due to the different preservation and occurrence of the taxa in the two sections, the distribution pattern of calcareous nannofossils was kept separated for the overlapping interval (Fig. 6).

The identification at specific level of the discoasters and the distribution pattern of small-sized helicoliths was performed only at the Castle section. *Helicosphaera walbersdorfensis* is generally common, but low percentage levels were found in the lowermost and uppermost part of the section. *Helicosphaera stalis* shows a scattered distribution and low percentages throughout.

Astronomical calibration of these events obtained by Lirer et al. (2002) and reported in Tab. 3 were compared with the ages, for the same biohorizons obtained in other Mediterranean sections (Malta Island: Foresi et al. 2002a; Sicily: Di Stefano et al. 2002, and in Equatorial Pacific (Shackleton et al. 1995).

Calcidiscus premacintyrei (Theodoridis)

Comments on this taxon have been reported by Foresi et al. (2002a). The distribution pattern of *C. premacintyrei* shows a clear drop in abundance in the Cemetery section in cycle 98. Above cycle 98, this taxon is extremely rare to absent. In the Castle section the abundance pattern of this taxon is discontinuous and reaches very low percentages (<2-3%).

As in other mainly terrigenous Mediterranean sequences (Fornaciari et al. 1996; Foresi et al. 2002a), it is very hard to establish if these rare occurrences are related to autochthonous or reworked specimens. The drop in abundance occurring in cycle 98 has been considered as the LCO of *C. premacintyrei*. The cyclostratigraphically calibrated age of this level is 12.51 Ma (see Tab. 3). This age is fully correlatable with the age obtained for the same biohorizon in the Malta section (Foresi et al. 2002a). The LCO biohorizon has been firstly utilized by Fornaciari et al. (1996) as zonal marker to detect the boundary between NN6-NN7 Zones of Martini (1971) in the Mediterranean Miocene record. The data reported here point out that this biohorizon can be considered isochronous and therefore, useful for time correlation in the Mediterranean. No estimated age for the LCO of *C. premacintyrei* has been reported in literature, but Shackleton et al. (1995) give an age of 12.65 Ma to a "*C. premacintyrei* top horizon" at low-latitude equatorial Pacific ODP Leg 138.

Taxa	Event	Cycle	Position(m)	Age
Planktonic foraminifera				
Neogloboquadrina atlantica atlantica	FO	34	36,39	11,16
Paragloborotalia siakensis	LO	37	34,49	11,21
Dentoglobigerina altispira spp.	LRO	50	30,01	11,47
Globigerinoides subquadratus	LCO	53	28,89	11,54
Globigerinoides obliquus obliquus	FRO	53	28,69	11,54
Neogloboquadrina acostaensis	FO	66	22,17	11,80
Neogloboquadrina atlantica praeatlantica	FO	66	22,17	11,80
Paragloborotalia partimlabiata	LO	66	22,17	11,80
Catapsydrax parvulus	FCO	66	22,17	11,80
Catapsydrax parvulus	FO	68	21,77	11,83
Dentoglobigerina altispira spp.	LCO	74	17,75	11,97
Paragloborotalia siakensis	AE	75	17,20	12,01
Paragloborotalia mayeri	LO	81	13,10	12,14
G. decoraperta gr.	FCO	81	13,10	12,14
Paragloborotalia mayeri	FCO	90	8,1	12,34
Paragloborotalia siakensis	AB	92	6,9	12,39
Calcareous nannofossils				
Coccolithus miopelagicus	LCO	35	35,29	11,18
Discoaster kugleri	LCO	56	27,29	11,60
Discoaster kugleri	FCO?	71	19,20	11,90
Calcidiscus macintyrei	FCO	90	8,2	12,34
Calcidiscus premacintyrei	LCO	98	3,6	12,51
Calcidiscus macintyrei	FO	101	1,7	12,57

Tab. 3 - Stratigraphic position and astronomical ages of calcareous plankton events.

Calcidiscus macintyrei (Loeblich & Tappan)

Comments on the taxonomic concept, quantitative distribution, occurrence and reliability of this taxon are reported by Foresi et al. (2002a), to whom the readers can refer to.

Generally, the *Calcidiscus* population is very scarce in the Cemetery section and in some samples, only a long search allowed us to obtain a total of 10 specimens of this genus. The high resolved distribution pattern of *C. macintyrei* shows that, even if discontinuously present, its first occurrence is slightly below the LCO of *C. premacintyrei* as in the Malta section. From the topmost part of cycle 90 it increases in abundance and is more continuously present upwards.

Fornaciari et al. (1996) did not use the FO of *C. macintyrei* for defining a zonal boundary due to the initial rarity. We suggest that this event could be used in the Mediterranean, even if not as a zonal boundary marker, to improve the stratigraphic resolution in the topmost part of the MNN6b Subzone. If the FO of this taxon is recognised by means of high resolution analyses, it can discriminate a very short stratigraphic interval below the LCO of *C. premacintyrei*. The time interval covered by the co-occurrence of these two taxa coincides with three precession cycles both in the Tremiti and in the Malta section (Foresi et al. 2002a). The cyclostratigraphically calibrated age of the FO of *C. macintyrei* in the S. Nicola composite section falls in cycle 101 at 12.57 Ma (Tab. 3) (Lirer et al. 2002). The same age has been obtained for this event in the Malta section (Foresi et al. 2002a). This Mediterranean age strongly differs from the age of 12.14 Ma reported by Shackleton et al. (1995) for their "*C. macintyrei* bottom horizon" at the low latitude equatorial Pacific Ocean. Therefore, its entry level in the Mediterranean record is older, confirming the biogeographical control on the distribution of this taxon.

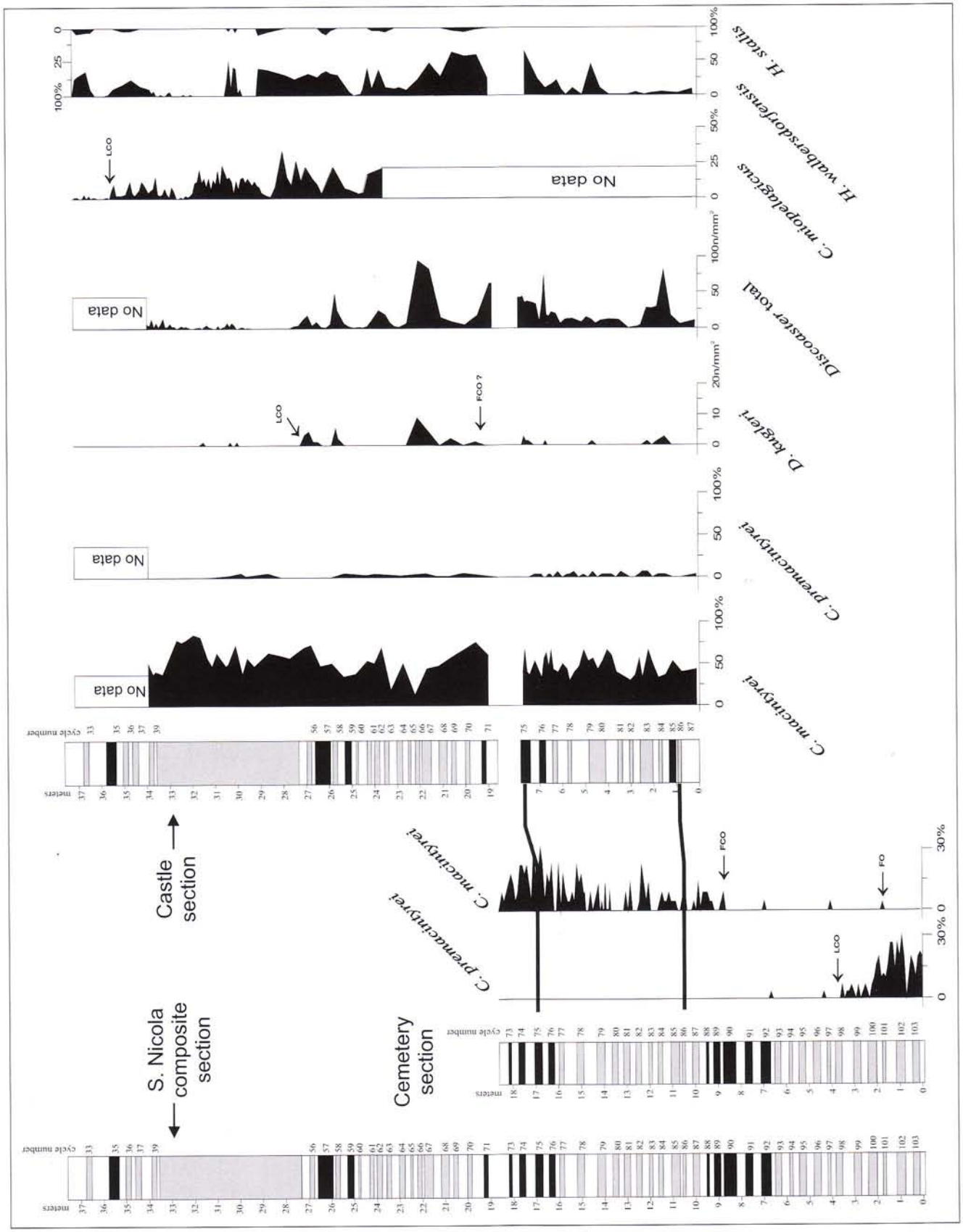

Fig. 6 - Quantitative distribution of selected calcareous nannofossils. FO: First Occurrence; FCO: First Common Occurrence; LCO: Last Common Occurrence.

PLATE 1

Fig. 1 - *Globigerinoides obliquus obliquus*: umbilical view, TTAA-298; Fig. 2 - *Globigerinoides obliquus obliquus*: lateral view, TTAA-298; Fig. 3 - *Globigerinoides obliquus obliquus*: spiral view, TTAA-298; Fig. 4 - *Globigerinoides subquadratus*: spiral view, TTAA-213; Fig. 5 - *Globigerinoides subquadratus*: lateral view, TTAA-213; Fig. 6 - *Globigerinoides subquadratus*: umbilical view, TTAA-213; Fig. 7 - *Neogloboquadrina acostaensis* s.s.: spiral view, TTAA-306; Fig. 8 - *Neogloboquadrina acostaensis* s.s: umblical view, TTAA-306; Fig. 9 - *Neogloboquadrina atlantica praeatlantica*: spiral view, TTAA-163; Fig. 10 - *Neogloboquadrina atlantica praeatlantica*: umbilical view, TTAA-163; Fig. 11 - *Neogloboquadrina atlantica praeatlantica*: lateral view, TTAA-173; Fig. 12 - *Neogloboquadrina atlantica praeatlantica*: spiral view, TTAA-173; Fig. 13 - *Neogloboquadrina atlantica praeatlantica*: umbilical view, TTAA-173; Fig. 14 - *Neogloboquadrina atlantica praeatlantica*: umbilical view, TTAA-173; Fig. 15 - *Neogloboquadrina atlantica praeatlantica*: spiral view, TTAA-292; Fig. 16 - *Neogloboquadrina atlantica praeatlantica*: lateral view, TTAA-292; Fig. 17 - *Catapsydrax parvulus*: umbilical view, TTAA-163; Fig. 18 - *Catapsydrax parvulus*: umbilical view, TTAA-173; Fig. 18 - *Globorotalia praemenardii praemenardii*: spiral view, TTAA-233; Fig. 20 - *Globorotalia praemenardii praemenardii*: umbilical view, TTAA-233;

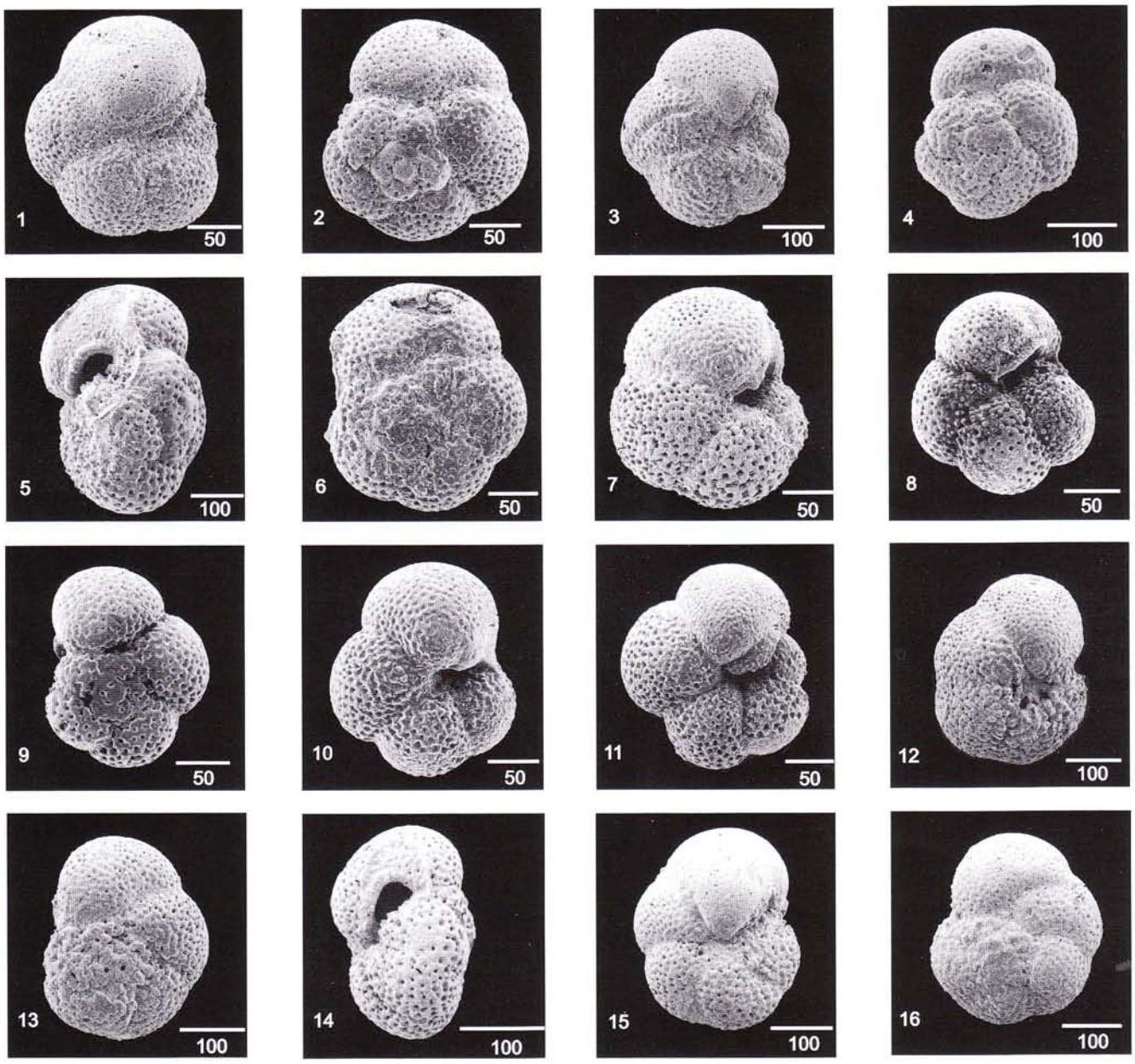

PLATE 2

Fig. 1 - *Paragloborotalia partimlabiata*: umbilical view, TTA-76; Fig. 2 - *Paragloborotalia partimlabiata*: spiral view, TTA-76; Fig. 3 - *Paragloborotalia partimlabiata*: umbilical view, TTA-89; Fig. 4 - *Paragloborotalia partimlabiata*: spiral view, TTA-89; Fig. 4 - *Paragloborotalia partimlabiata*: lateral view, TTAA-119; Fig. 6 - *Paragloborotalia partimlabiata*: spiral view, TTAA-119; Fig. 7 - *Paragloborotalia partimlabiata*: umbilical view, TTAA-119; Fig. 8 - *Paragloborotalia* cf. *partimlabiata*: spiral view, TTAA-213; Fig. 9 - *Paragloborotalia* cf. *partimlabiata*: umbilical view, TTAA-215; Fig. 10 - *Paragloborotalia* cf. *partimlabiata*: umbilical view, TTAA-215; Fig. 11 - *Paragloborotalia* cf. *partimlabiata*: umbilical view, TTAA-215; Fig. 12 - *Paragloborotalia mayeri*: umbilical view, TTA-86; Fig. 13 - *Paragloborotalia mayeri*: spiral view, TTA-86; Fig. 14 - *Paragloborotalia mayeri*: lateral view, TTA-86; Fig. 15 - *Paragloborotalia mayeri*: umbilical view, TTAA-39; Fig. 16 - *Paragloborotalia mayeri*: spiral view, TTAA-39.

Above cycle 90 higher percentage values and a more regular occurrence can be detected up to the top of the Cemetery section. We tentatively consider the beginning of this abundance increase as a distinctive FCO horizon in the quantitative distribution of the taxon. Its astrochronological age is 12.34 Ma (Tab. 3). In the Castle section, the *Calcidiscus* population is well represented and preserved; a continuous occurrence of *C. macintyrei*, with percentage values ranging from 20 to 90%, was detected in samples studied every 20 cm.

Discoaster kugleri (Martini & Bramlette)

To identify *Discoaster kugleri*, the original description reported by Martini & Bramlette (1963) has been strictly followed. The poor preservation of the *Discoaster* population in the Cemetry section hampered the

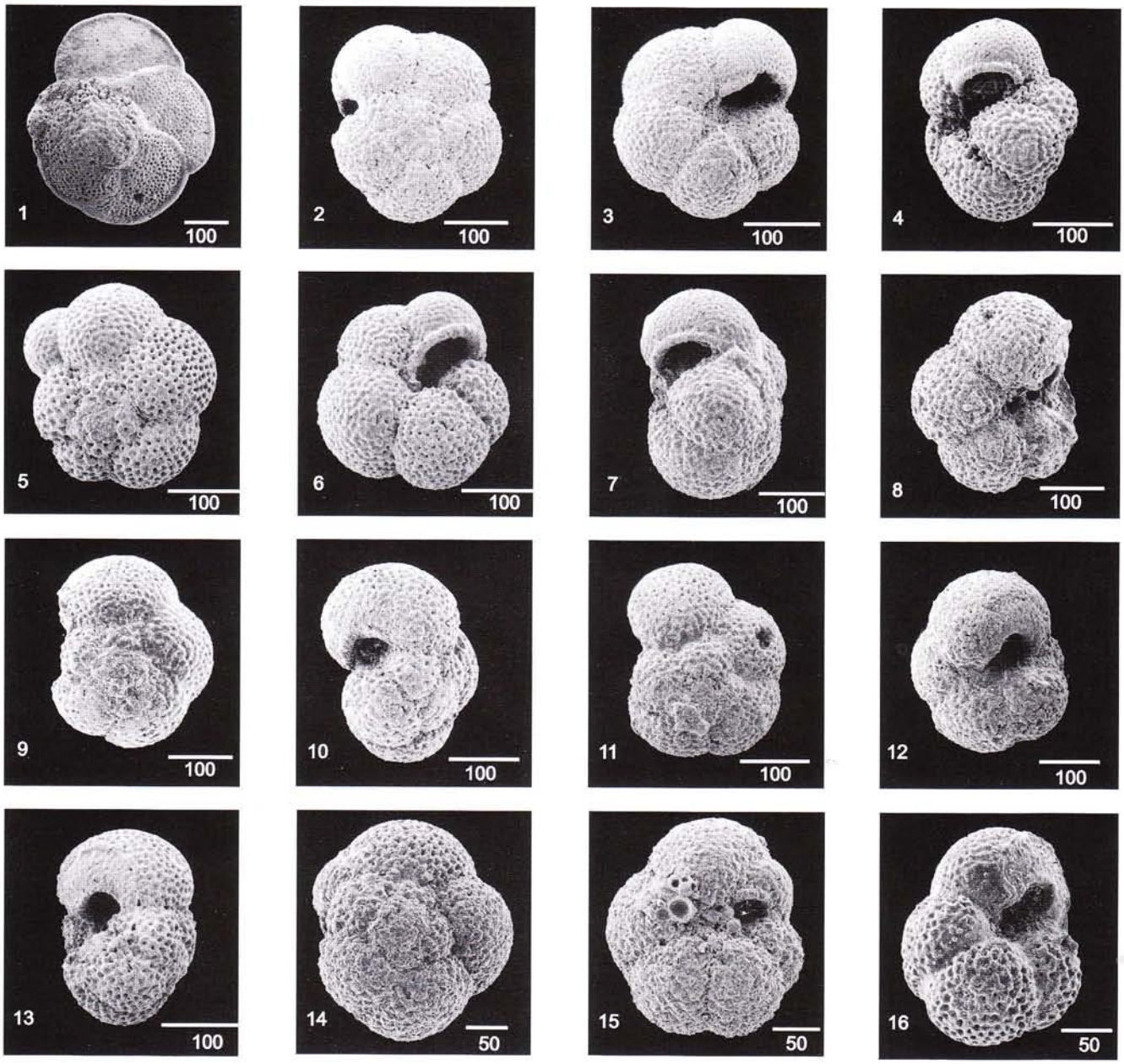

PLATE 3

Fig. 1 - *Globorotalia* aff. *menardii*: spiral view, TTAA-223; Fig. 2 - *Paragloborotalia siakensis*: spiral view, TTA-103; Fig. 3 - *Paragloborotalia siakensis*: umbilical view, TTA-103; Fig. 4 - *Paragloborotalia siakensis*: lateral view, TTA-103; Fig. 5 - *Paragloborotalia siakensis*: spiral view, TTA-101; Fig. 6 - *Paragloborotalia siakensis*: umbilical view, TTA-101; Fig. 7 - *Paragloborotalia siakensis*: lateral view, TTA-101; Fig. 8 - *Paragloborotalia siakensis*: umbilical view, TTAA- 59; Fig. 9 - *Paragloborotalia siakensis*: spiral view, TTAA-59; Fig. 10 - *Paragloborotalia siakensis*: lateral view, TTAA-59; Fig. 11 - *Paragloborotalia siakensis*: spiral view, TTAA-103; Fig. 12 - *Paragloborotalia siakensis*: umbilical view, TTAA-103; Fig. 13 - *Paragloborotalia siakensis*: lateral view, TTAA-103; Fig. 14 - *Paragloborotalia siakensis*: spiral view, TTAA-233; Fig. 15 - *Paragloborotalia siakensis*: umbilical view, TTAA-233; Fig. 16 - *Paragloborotalia siakensis*: umbilical view, TTAA-278;

recognition of the distribution of *D. kugleri*. In the Castle section the discoasterids are better represented and preserved, and a detailed study was carried out to obtain the distribution pattern of *D. kugleri*. Nevertheless, this pattern is difficult to interpret because *D. kugleri* is randomly present in the lower part of the section and shows more continuous presence from cycle 71. The distribution pattern of the taxon is missing in the interval from cycle 74 to cycle 72 because of the presence of the above mentioned shear plane (Fig. 6).

We tentatively place the FCO of *D. kugleri* in cycle 71 of the Castle section at an astronomical age of 11.90 Ma. This age is in agreement with the age of the lithologic cycle where the FCO of the species has been identified by Hilgen et al. (2000).

Between cycles 71 and 56, *D. kugleri* shows fluc-

tuating abundance and discontinuous occurrence, with a maximum of 10 specimens per mm^2 within cycle 67. The highest values coincide with high frequencies of the total *Discoaster* distribution as also observed in the Case Pelacani section (Di Stefano et al. 2002).

The *D. kugleri* LCO is located in coincidence of the significant drop in its relative abundance within cycle 56, dated at 11.60 Ma. This age is in good agreement with that obtained for the same biohorizon in the Gibliscemi record (Hilgen et al. 2000) and in the Case Pelacani section (Di Stefano et al. 2002). The highest occurrence of the species was detected at level 31.5 m, but it is hard to establish if this represents the real extinction level of the taxon.

Fornaciari et al. (1996) attribute to this form a limited biostratigraphic potential, pointing out the difficulty of recognising the range of *Discoaster kugleri* in the Miocene Mediterranean record where it is poorly represented. Hilgen et al. (2000), however, show a clear biostratigraphic signal provided by *D. kugleri* distribution in the Gibliscemi section and propose a *Discoaster kugleri* Subzone within the MNN7 Biozone of Fornaciari et al. (1996) defined by the FCO and LCO of this form.

Coccolithus miopelagicus (Bukry)

Coccolithus miopelagicus is an easily detectable and well represented form both in the Mediterranean and in oceanic regions. The biostratigraphic value of the LO of *C. miopelagicus* is worldwide used although a slight diachroneity for this event exists between low and mid latitude (Raffi et al. 1995; Backman & Raffi 1997). In the Mediterranean, Fornaciari et al. (1996) recorded the LCO of *C. miopelagicus*, just below the LO of *H. walbersdorfensis*, but they did not use the bioevent in their zonal scheme.

In the Castle section *C. miopelagicus* shows a saw teeth distribution pattern through the considered interval (quantitative analyses on this taxon have been performed only from cycle 62 upsection) and it becomes extremely rare in the topmost levels. In the upper part of *C. miopelagicus* range, an absence or very low-frequency ("paracme") occurs in a very short interval between 32 and 33 meters; the same feature has been detected in the distribution pattern reported for this taxon at Case Pelacani section (Di Stefano et al. 2002). We located the LCO of *C. miopelagicus* close to the highest significant drop of frequency of the taxon at 35.29 m, dated at 11.18 Ma, in agreement with the age recorded in the Case Pelacani section (Di Stefano et al. 2002).

Serravallian/Tortonian boundary

The Serravallian/Tortonian (S/T) boundary historically slighty predates the FO of *N. acostaensis* (Cita & Blow 1969). However this event was supposed to occur from the basal part of the Tortonian stratotype section of Rio Mazzapiedi-Castellania (Cita & Premoli Silva 1968). In the low latitude zonal scheme of Blow (1969), this event defines the N15/N16 boundary and occurs later than the LO of *P. siakensis* which defines the N14/N15 boundary and therefore the two events are far each other. At middle latitudes (Miller et al. (1985, 1991, ODP Site 608) these events occur very close to each other. Partial overlaps in the range of the two taxa are recorded by Cita et al. 1965, Mazza 1985; Coccioni et al. 1992; Foresi 1993; Foresi et al. 1998 in the Mediterranean and by Huddleston (1984) in the North Atlantic. According to Zachariasse (1992) *N. acostaensis* migrated to the tropical area from high latitude. This migration to the low latitude (Ceara Rise, ODP Leg 154) was dated through astronomical tuning by Chaisson & Pearson (1997) at 9.82 Ma and by Turco et al. (in press) at 9.89 Ma. In the Mediterranean area, Foresi et al. (1998) estimated for the FO of *N. acostaensis* and LO of *P. siakensis* respectively an age of 11.5 Ma and 10.5 Ma while Hilgen et al. (2000), using astronomical tuning, dated the entry of the neogloboquadrinids at 11.78 Ma and the exit of *P. mayeri* (= *P. siakensis* of this paper) at 11.21 Ma. Therefore, the overlap between the two taxa lasts about 600 kys, At low latitude, the entry of *N. acostaensis* postdates the exit of *P. siakensis* of 540 kys (Turco et al. in press). The arrival of *N. acostaensis* is delayed of almost 2 milions years in low latitudes compared with the Mediterranean.

The S/T boundary in the Tortonian stratotype based on calcareous nannofossils is conflicting compared with those of the planktonic foraminifera. In fact, the boundary occurs within zone NN9 in Mazzei (1977) or NN8 in Rio et al. (1997), whereas according to Foresi et al. (1998), Hilgen et al. (2000) and our data, the *N. acostaensis* FO falls within NN7, indicating that the base of the Tortonian stratotype postdates the *N. acostaensis* FO. Foresi et al. (1998) and Hilgen et al. (2000) indicate that the base of the Tortonian stratotype approximates the FRO of *N. acostaensis*. Therefore, the GSSP of the Tortonian should be placed within the FO and FRO of *N. acostaensis*. The LCO of *G. subquadratus* at 11.54 Ma could be a potential candidate for the GSSP of the Tortonian for its synchroneity between Mediterranean and low latitude oceans as reported in Turco et al. (in press).

Conclusions

The highly detailed micropaleontological study of the composite Middle Miocene section of the Tremiti Islands, allowed us to display the quantitative distribution pattern of the most significant calcareous plankton taxa of the Late Serravallian. The section has been astronomically calibrated by Lirer et al. (2002) and it spans the interval between 12.61-11.12 Ma. All the recognised

bioevents have been astrochronologically dated. The stratigraphic positions and the astronomical ages are shown in Tab. 3. Several bioevents and their position are in good agreement with those recently recorded by Hilgen et al. (2000), rendering them strongly reliable for biostratigraphic use.

From a chronostratigraphic point of view the S. Nicola composite section belongs to the Serravallian time interval. Only the upper part could be assigned to the Tortonian depending on the criteria which will be adopted for the GSSP of the Tortonian.

Acknowledgements. We are grateful to I. Premoli Silva and K. Von Salis and for a critical review of the manuscript. This work was supported financially by Ministero della Università e della Ricerca scientifica e Tecnologica (MURST COFIN '98).

REFERENCES

Backman J. & Raffi I. (1997) - Calibration of Miocene nannofossil events to orbitally tuned cyclostratigraphies from Ceara Rise. In Shackleton N.J., Curry W.B., Richter C. & Bralower T.J. (Eds.) *Proc. ODP, Sci. Results*, 154: 83-99, College Station (TX).

Backman J. & Shackleton N.J. (1983) - Quantitative biochronology of Pliocene and early Pleistocene calcareous nannofossils from the Atlantic, Indian and Pacific oceans. *Mar. Micropaleontology*, 8: 141-170, Amsterdam.

Baldacci O. (1953) - Ricerche geografiche sulle isole Tremiti. *Boll. Soc. Geogr. It.*, 6: 431-410, Roma.

Bassani F. (1907) - Su alcuni avanzi di pesci nell'arenaria glauconiosa delle Isole Tremiti. *Rend. R. Acc. Sc. Fis. Mat. Napoli*, 46: 156-160, Napoli.

Berggren W.A., Hilgen F.J., Langereis C.G., Kent D.V., Obradovich J.D., Raffi I., Raymo M.E. & Shackleton N.J. (1995) - Late Neogene (Pliocene-Pleistocene) Chronology: New perspectives in high resolution stratigraphy. *Geol. Soc. Am. Bull.*, 107: 1272-1287, Boulder, Colorado.

Blow W.H. (1969) - Late Middle Eocene to Recent planktonic foraminiferal biostratigraphy. In: Brönnimann P. & Renz H.H. (eds.). *Proc. First. Int. Conf. Plankt. Microf.*, Geneva 1967, 1:199-421, Leiden.

Bolli H.M. & Saunders J.B. (1982) - *Globorotalia mayeri* and its relationship to *Globorotalia siakensis* and *Globorotalia continuosa*. *Journ. Foram. Res.*, 12(1): 39-50, Washington.

Bolli H.M. & Saunders J.B. (1985) - Oligocene to Holocene low latitude planktic foraminifera. In: Bolli H.M. et. (eds.) - Plankton stratigraphy. 1: 155-262, Cambridge University Press.

Bossio A., Iaccarino S., Mazzei R., Monteforti B., Salvatorini G. & Tanzi F. (1992) - Miocene calcareous plankton biostratigraphy of the Tremiti Islands (Southern Adriatic Sea). In: Montanari A. et al. (eds.) - Conferenza interdisciplinare di geologia sull'epoca miocenica con enfasi sulla sequenza umbro-marchigiana, Ancona 1992, *I.U.G.S. Miocene Columbus Project*, Abstract, and field trips 27.

Chaisson W.P. & Pearson P. N. (1997) - Planktonic foraminifer biostratigraphy at Site 925: Middle Miocene - Pleistocene. In: Curry W.B., Shackleton N.J., Richter C. & Bralower T.J. (eds.). *Proc. ODP, Sci. Results*: 154: 3-31, College Station (TX).

Checchia Rispoli G. (1926) - Osservazioni geologiche sull'Isola di S. Nicola di Tremiti (Mare Adriatico). *Boll. R. Uff. Geol. Ital.*, 51: 1-3, Roma.

Checchia Rispoli G. (1928) - Su di una nuova Chlamys (C. adriatica) del Miocene delle isole Tremiti. *Boll. R. Uff. Geol. Ital.*, 53: 1-4, Roma.

Cita M.B. & Blow W.H. (1969) - The biostratigraphy of the Langhian, Serravallian and Tortonian Stages in the Type Section in Italy. *Riv. Ital. Paleont. Strat.*, 75: 549-603, Milano

Cita M.B., Colalongo M.L., D'Onofrio S., Iaccarino S. & Salvatorini G. (1978) - Biostratigraphy of Miocene deep-sea sediments (Sites 372 and 375), with special reference to the Messinian/pre-Messinian interval. In: Hsü K., Montadert L. et al. (eds.). *Init. Rep. DSDP*, 42: 671-685, Washington (U.S. Government Printing Office).

Cita M.B. & Premoli Silva I. (1968) - Evolution of the planktonic foraminiferal assemblages in the stratigraphic interval between the type-Langhian and the type-Tortonian and biozonation of the Miocene of the Piedmont, *Giorn. Geol.*, 35(3): 1-28, Bologna.

Cita M.B., Premoli Silva I. & Rossi R. (1965) - Foraminiferi planctonici del Tortoniano tipo. *Riv. Ital. Paleont. Strat.*, 71: 217-308, Milano.

Coccioni R., Di Leo C. & Galeotti S. (1992) - Planktonic foraminiferal biostratigraphy of the upper Serravallian - lower Tortonian Monte dei Corvi Section (Northeastern Apennines, Italy). In: Montanari A. et al.(eds.) - Conferenza interdisciplinare di geologia sull'epoca miocenica con enfasi sulla sequenza umbro-marchigiana, Portonove Ancona 1992, *Miocene Columbus Project* (I.U.G.S). Abstracts and field trips, 53-56.

Cotecchia V., Guerricchio A. & Melidoro G. (1996) - Geologia e processi di demolizione costiera dell'Isola di S. Nicola (Tremiti). *Mem. Soc. Geol. It.*, 51: 595-606, Roma.

Di Stefano E. (1998) - Calcareous nannofossil quantitative biostratigraphy of Holes 969E and 963B (Eastern Mediterranean). In: Robertson A.H.F., Emeis K.C., Richter C. & Camerlenghi A. (eds). *Proc. ODP, Sci. Results*, 160: 99-112, College Station (TX).

Di Stefano E., Bonomo S., Caruso A., Dinarés-Turell J., Foresi L.M., Salvatorini & Sprovieri R. (2002) - Calcareous

plankon bio-events in the Miocene Case Pelacani section (south-eastern Sicily, Italy). In: Iaccarino S.M. (ed.) - Integrated Stratigraphy and Paleoceanography of the Mediterranean Middle Miocene. *Riv. It. Paleont. Strat.*, 108: 307-324, Milano.

Foresi L.M. (1993) - Biostratigrafia a foraminiferi planctonici del Miocene medio del Mediterraneo e delle basse latitudini con considerazioni cronostratigrafiche. *PhD. thesis*, Parma University: 1-143, Parma.

Foresi L.M., Iaccarino S., Mazzei R. & Salvatorini G. (1998) - New data on middle to late Miocene calcareous plankton biostratigraphy in the Mediterranean area. *Riv. Ital. Paleont. Strat.*, 104: 95-114, Milano.

Foresi L.M., Bonomo S., Caruso A., Di Stefano E., Salvatorini G., Sprovieri R., (2002a) - Calcareous plankton high resolution biostratigraphy (foraminifera and nannofossils) of the uppermost Langhian-lower Serravallian Ras Il-Pellegrin section (Malta). In: Iaccarino S.M. (ed.) - Integrated Stratigraphy and Paleoceanography of the Mediterranean Middle Miocene. *Riv. It. Paleont. Strat.*, 108: 195-210, Milano

Foresi L.M., Iaccarino S., Mazzei R., Salvatorini G. & Bambini A.M. (in press) - Il plancton calcareo (foraminiferi e nannofossili) del Miocene delle Isole Tremiti. *Palaeont. Ital.*, Pisa.

Foresi L.M., Iaccarino S. & Salvatorini G. (2002 b) - *Neogloboquadrina atlantica praeatlantica*, new subspecies from late Middle Miocene. In: Iaccarino S.M. (ed.) - Integrated Stratigraphy and Paleoceanography of the Mediterranean Middle Miocene. *Riv. It. Paleont. Strat.*, 108: 325-336, Milano.

Fornaciari E., Di Stefano A., Rio D. & Negri A. (1996) - Middle Miocene quantitative calcareous nannofossil biostratigraphy in the Mediterranean region. *Micropaleontology*, 42: 37-63, New York.

Gambini R. & Tozzi M. (1996) - Tertiary geodynamic evolution of the Southern Adria microplate. *Terra Nova*, 8: 593-602, Oxford.

Giannelli L. & Salvatorini G. (1975) - I Foraminiferi dei sedimenti dell'Arcipelago maltese. II. Biostratigrafia di: "Blue Clay", "Greensand" e "Upper Coralline Limestone". *Atti Soc. Tosc. Sc. Nat. Mem.*, 82: 1-24, Pisa.

Hilgen F.J. (1991a) - Astronomical calibration of Gauss to Matuyama sapropels in the Mediterranean and implication for Geomagnetic Polarity Time Scale. *Earth Plan. Sci. Lett.*, 104: 226-244, Amsterdam.

Hilgen F.J. (1991b) - Extension of the astronomically calibrated (polarity) time scale to the Miocene/Pliocene boundary. *Earth Plan. Sci. Lett.*, 107: 349-368, Amsterdam.

Hilgen F.J., Krijgsman W., Langereis C.G., Lourens L.J., Santarelli A. & Zachariasse W.J. (1995) - Extending the astronomical (polarity) time scale into the Miocene. *Earth Plan. Sci. Lett.*, 136: 495-510, Amsterdam.

Hilgen F.J., Krijgsman W., Raffi I., Turco E. & Zachariasse W.J. (2000) - Integrated stratigraphy and astronomical calibration of the Serravallian/Tortonian boundary section at Monte Gibliscemi (Sicily, Italy). *Marine Micropaleontology*, 38: 181-211, Amsterdam.

Huddleston P.F. (1984) - Planktonic foraminiferal biostratigraphy, Deep Sea Drilling Project Leg 81 In: Roberts D.G., Schnitker D. et al. (eds.). *Init. Reports DSDP*, 81: 429-438, Washington (U.S. government Printing Office).

Iaccarino S. (1985) - Mediterranean Miocene and Pliocene planktic foraminifera. In: Bolli H.M. Saunders J.B & Perch Nielsen K. (eds.) - *Plankton Stratigraphy*, 1: 283-314, Cambridge University Press.

Iaccarino S., Foresi L.M, Mazzei R. & Salvatorini. (2001) - Calcareous plankton biostratigraphy of the Miocene sediments of the Tremiti Islands (Southern Italy). *Rev. Españ. Micropal*, 33(2): 237-248, Madrid.

Iaccarino S. & Salvatorini G. (1982) - A framework of planktonic foraminiferal biostratigraphy for Early Miocene to Late Pliocene Mediterranean area. *Paleont. Stratigr. Evoluz.*, 2: 115-125, Roma.

Krijgsman W., Hilgen F.J., Langereis C.G., Santarelli A. & Zachariasse W.J. (1995) - Late Miocene magnetostratigraphy, biostratigraphy and cyclostratigraphy in the Mediterranean. *Earth Plan. Sci. Lett.*, 136: 475-494, Amsterdam.

Krijgsman W., Langereis C.G., Zachariasse W.J., Boccaletti M., Moratti G., Gelati R., Iaccarino S., Papani G., Villa G. (1999) - Late Neogne evolution of the Taza-Guercif Basin (Rifian Corridor, Morocco) and implications for the Messinian salinity crisis. *Mar. Geology*, 153:147-160, Amsterdam.

Laskar J., Joutel F. & Boudin F. (1993) - Orbital, precessional, and insolation quantities for the Earth from -20 Myr to +10 Myr. *Astron. Astrophys.*, 270: 522-533, Washington.

Lirer F., Caruso A., Foresi L.M., Sprovieri M., Bonomo S., Di Stefano A., Di Stefano E., Iaccarino S. M., Salvatorini G., Sprovieri R., Mazzola S. (2002) - Astrochronological calibration of the Upper Serravallian/Lower Tortonian sedimentary sequence at Tremiti Islands (Adriatic Sea, Southern Italy). In: Iaccarino S.M. (ed.) - Integrated Stratigraphy and Paleoceanography of the Mediterranean Middle Miocene. *Riv. It. Paleont. Strat.*, 108: 241-256, Milano.

Mazza P. (1985) - On the occurrence of *Neogloboquadrina acostaensis* in the upper Serravallian sediments of Sicily. *Riv. Ital. Paleont. Strat.*, 91: 513-518, Milano.

Mazzei R. (1977) - Biostratigraphy of the Rio Mazzapiedi - Castellania section (type-section of the Tortonian) based on calcareous nannoplankton. *Atti Soc. Tosc. Sc. Nat., Mem.*, Ser. A, 84, 15-24, Pisa.

Martini E. (1971) - Standard Tertiary and Quaternary calcareous nannoplankton zonation. In: Farinacci A. (ed.). *Proc. II Plankt. Confer.*, 1970, 738-785, Roma.

Martini E. & Bramlette M.N. (1963) - Calcareous nannoplankton from the experimental Mohole drilling. *Journ. Pal.*, 37 (4): 845-856, Tulsa.

Miller K.G., Aubry M.P., Khan M.J., Melillo A.J., Kent D.V. & Berggren W.A. (1985) - Oligocene-Miocene biostratigraphy, magnetostratigraphy and isotopic stratigraphy of western North Atlantic. *Geology*, 13: 257-261, Boulder.

Miller K.G., Feigenson M.D., Wright J.D. & Clement B.M. (1991) - Miocene isotope reference section, Deep Sea Drilling Project Site 608: an evaluation of isotope biostratigraphic resolution. *Paleoceanography*, 6: 33-52, Washington.

Pampaloni M.L. (1988) - Il Paleogene-Neogene delle Isole Tremiti (Puglia, Italia meridionale): stratigrafia ed analisi paleoambientale. *PhD. thesis*, V. of 183 pp., Roma.

Pasa A. (1953) - Appunti geologici per la paleogeografia delle

Puglie. *Mem. Biogeogr. Adriatica*, 2: 175-286.

Perch-Nielsen K. (1985) - Cenozoic calcareous nannofossils. In: Bolli H. M., Sanders J.B. and Perch-Nielsen K., (eds.) - Plankton Stratigraphy. 427-554. Cambridge University Press.

Raffi I. & Flores J.A. (1995) - Pleistocene through Miocene calcareous nannofossils from Eastern Equatorial Pacific Ocean (LEG 138). In: Pias N.G., Mayer L.A., et al. (eds.). *Proc. ODP, Sci. Results*, 138: 233-286, College Station (TX).

Raffi I., Rio D., d' Atri A., Fornaciari E. & Rocchetti S. (1995) - Quantitative distribution patterns and biomagnetostratigraphy of middle and late Miocene calcareous nannofossils from equatorial Indian and Pacifics oceans (Legs 115, 130 and 138). In: Pias N.G., Mayer L.A., et al. (eds.). *Proc. ODP Sci. Results*, 138: 479-502, College Station (TX).

Rio D., Cita M.B., Iaccarino S., Gelati R. & Gnaccolini M. (1997) - Langhian, Serravallian, and Tortonian historical stratotypes. In Montanari A., Odin G.S. & Coccioni R. (eds.) - *Miocene Stratigraphy: An Integrated Approach, Development in Paleontology and Stratigraphy*, 15: 57-87, Elsevier, Amsterdam.

Rio D., Raffi I. & Villa G. (1990) - Pliocene-Pleistocene calcareous nannofossil distribution patterns in the Western Mediterranean. In: Kastens K.A., Mascle J. et al. (eds.). *Proc. ODP, Sci. Results*, 107: 513-533, College Station (TX).

Salvatorini G. & Cita M.B. (1979) - Miocene foraminiferal stratigraphy, DSDP site 397 (Cape Bojader, North Atlantic) In: Ryan W.B.F. et al. (eds). *Init. Rep. Deep Sea Drilling Project*, 47 (1): 317-373, Washington.

Selli R. (1971) - Isole Tremiti e Pianosa. In: Cremonini et al. - S.Marco in Lamis. *Note Illustr. Carta Geol. d'Italia* scala *1:100.000*, Roma.

Shackleton N.J., Baldauf J.G., Flores A., Iwai M., Moore Jr., Raffi I. & Vincent E. (1995) - Biostratigraphic summary for LEG 138.). In: Pias N.G., Mayer L.A., et al. (eds.). *Proc. ODP, Sci. Results*, 138, 517-536. College Station (TX).

Shackleton N.J. & Crowhurst S. (1997) - Sediment fluxes based on orbital tuned time scale 5 MA to 14 MA, site 926. In: Shackleton N.J., Curry W.B., et al. (eds.) *Proc. ODP, Sci. Results*, 154: 69-82, College Station (TX).

Spiegler D. (1999) - *Bolboforma* biostratigraphy from the Hatton-Rockall Basin (North Atlantic). In: Raymo M.E., Jansen E., Blum P. & Herbert T.D. (eds.). *Proc. ODP, Sci. Results*, 162: 35-49, College Station (TX).

Sprovieri R., Bonomo S., Caruso A., Di Stefano A., Di Stefano E., Foresi L.M., Iaccarino S.M., Lirer F., Mazzei R., Salvatorini G. (2002) - An integrated calcareous plankton biostratigraphic scheme and biochronology for the Mediterranean Middle Miocene. In: Iaccarino S.M. (ed.) - Integrated Stratigraphy and Paleoceanography of the Mediterranean Middle Miocene. *Riv. It. Paleont. Strat.*, 108: 337-353, Milano.

Squinabol S. (1908) - Riassunto di uno studio geo-fisico sulle Tremiti. *Atti R. Acc. Sc.*, 43: 1008-1013, Roma.

Tellini A. (1890) - Osservazioni geologiche sulle Isole Tremiti e sull'Isola di Pianosa nell'Adriatico. *Boll. R. Com. Geol. It.*, 21: 442-514, Roma.

Tjalsma R.C. (1971) - Stratigraphy and foraminifera of the Neogene of the Eastern Guadalquivir Basin (southern Spain). *Utrecht Micropal. Bull.*, 4: 1-161, Utrecht.

Turco E., Foresi L.M., Lirer F., Iaccarino S.& Salvatorini G. (2001) - Middle Miocene biostratigraphy and Paleogeography fron the Equatorial Atlantic Ocean (Leg 154, Site 926A). International Conference, Paleobiogeography and Paleoecology. Piacenza (Abstract).

Turco E., Bambini A.M., Foresi L.M., Iaccarino S., Lirer F., Mazzei R. & Salvatorini G. (in press) - Middle Miocene high-resolution calcareous plankton biostratigraphy at Site 926 (Leg 154, equatorial Atlantic Ocean): paleoecological and paleobiogeographical implications. *Geobios* (special volume), Lyon.

Zachariasse W.J. (1975) - Planktonic foraminiferal biostratigraphy of the Late Neogene of Crete (Greece). *Utrecht Micropal. Bull.*, 11: 1-171, Utrecht.

Zachariasse W.J. (1992) - Neogene planktonic foraminifers from Sites 761 e 762 off Northwest Australia. In: Von Rad U. et al. (eds). *Proc. ODP., Sct. Res.*, 122: 665-675, College Station (TX).